

Connecting Dark Matter Annihilation to the Charge Radii of Standard Model Fermions

Jason Kumar^{1,*} and Christopher Light^{1,†}

¹*Department of Physics & Astronomy,
University of Hawaii, Honolulu, HI 96822, USA.*

Abstract

We consider scenarios in which dark matter is a Majorana fermion which couples to Standard Model fermions through the exchange of charged mediating particles. The matrix elements for various dark matter annihilation processes are then related to one-loop corrections to the fermion-photon vertex, where dark matter and the charged mediators run in the loop. In particular, in the limit where Standard Model fermion helicity mixing is suppressed, the cross section for dark matter annihilation to various final states is related to the corrections to Standard Model fermion charge radii. Although current measurements of the charge radii are not precise enough to provide useful constraints on dark matter annihilation, improved measurements at future experiments, such as the International Linear Collider, could improve these constraints by several orders of magnitude, allowing them to surpass the limits obtainable by direct observation.

arXiv:1612.00773v1 [hep-ph] 2 Dec 2016

* jkumar@hawaii.edu

† lightc@hawaii.edu

1. INTRODUCTION

It has long been appreciated that if dark matter (DM) is a Majorana fermion and if the theory respects minimal flavor violation (MFV), then dark matter annihilation to light Standard Model (SM) fermions is p -wave suppressed in the chiral limit. Nevertheless, p -wave annihilation can be an important process in the early Universe during the epoch of thermal dark matter freeze-out, when this velocity-suppression is only an $\mathcal{O}(0.1)$ effect. In the current epoch, when this velocity suppression is large ($\sim 10^{-6}$), indirect detection signals may instead be dominated by other annihilation processes, such as virtual internal bremsstrahlung (IB), or annihilation to photons via a one-loop diagram. In this work, we consider the constraints on these annihilation processes which can arise from associated corrections to the charge radii of the Standard Model fermions.

If dark matter (χ) annihilates to charged SM fermions (f) through the t -channel exchange of charged mediating particles, then there is necessarily a one-loop correction to the fermion-photon vertex arising from diagrams where χ and the charged mediators run in the loop (see Figure 1). It has previously been shown [1] that the s -wave dark matter annihilation matrix element is directly correlated with the associated correction to the electric and magnetic dipole moments of the SM fermions. This connection follows from general principles: the annihilation process $\chi\chi \rightarrow \bar{f}f$ can only proceed from an s -wave initial state if there is some mixing of SM fermion helicities, and the electromagnetic form factors which contribute to helicity mixing yield the electric and magnetic dipole moments in the limit of small momentum transfer. One might expect that the annihilation matrix elements which do not mix SM fermion Weyl spinors can be similarly correlated with corrections to the electromagnetic form factors which do not mix SM fermion Weyl spinors, and we will see that this is indeed the case. In particular, these annihilation matrix elements can be related to the correction to the fermion charge radius, which parameterizes the correction to the helicity-preserving form factor in the limit of small momentum transfer.

Corrections to the charge radii of SM charged fermions are constrained by measurements at LEP [2], and future experiments may yield much more precise measurements. We will find that these constraints can be translated into bounds on the non-helicity-mixing terms of the cross sections for the dark matter annihilation processes $\chi\chi \rightarrow \bar{f}f, \bar{f}f\gamma, \gamma\gamma$. But experiments constrain the total correction to the fermion charge radius, which can arise both from diagrams involving dark matter, as well as from new physics unrelated to dark matter. Thus, it is always possible that a large correction to the charge radius arising from loop corrections involving dark matter could be canceled by another large correction arising from unrelated new physics, leaving a small total

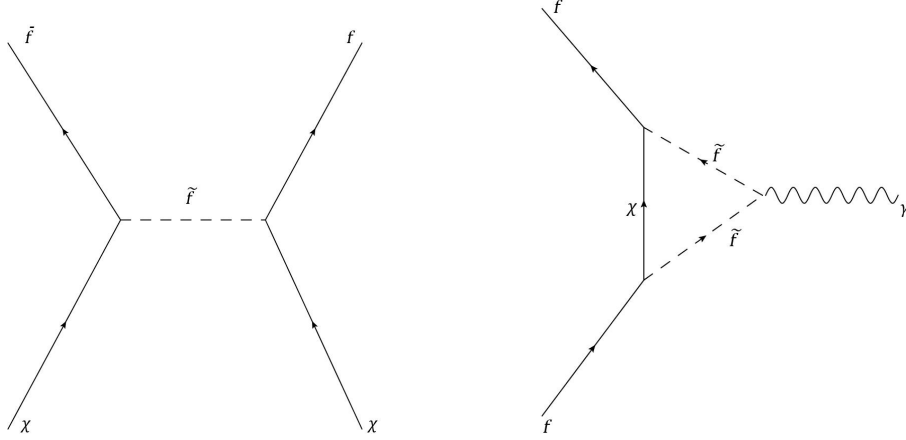


FIG. 1: Feynman diagrams corresponding to the annihilation process $\chi\chi \rightarrow \bar{f}f$ (left diagram) and to the correction to the fermion-photon vertex (right diagram).

correction to the charge radius. As a result, the constraints we will find, at a rigorous level, really indicate the extent to which one must fine-tune different corrections to the charge radius in order to retain consistency with the data.

We will see that current bounds from LEP are not precise enough to be useful. But future analyses, particularly using colliders with higher energy and luminosity than LEP, could provide much better measurements of SM fermion charge radii, potentially improving the resulting constraints on dark matter annihilation processes by several orders of magnitude. In this case, the resulting constraints could not only be relevant for constraining models of dark matter annihilation in the early Universe, but could exceed limits obtainable in the current epoch from direct observation.

The plan of this paper is as follows. In Section 2, we describe the relationship between the SM fermion charge radius correction and the annihilation cross sections for the processes $\chi\chi \rightarrow \bar{f}f, \bar{f}f\gamma, \gamma\gamma$. In section 3, we determine the constraints imposed on dark matter annihilation from current and potential measurements of the SM fermion charge radii, both in the early Universe and in the present epoch. We conclude in section 4 with a discussion of our results.

2. CONNECTING DARK MATTER ANNIHILATION TO THE FERMION VERTEX CORRECTION

We first consider the scenario in which a Majorana fermion dark matter particle (χ) annihilates to a SM charged fermion/anti-fermion pair ($\bar{f}f$) through the t -channel exchange of mediating particles, which necessarily are also charged.

The suppression of the s -wave annihilation cross section in the chiral limit ($m_f/m_\chi \rightarrow 0$) can

be understood from the conservation of angular momentum (see, for example, [3]). Since the initial state consists of two identical fermions, it must be totally anti-symmetric, implying that the $L = 0$ initial state must also have $S = 0$, $J = 0$. The $\bar{f}f$ final state must then also have $J_z = 0$, where we take the z -axis to be the direction of motion of the outgoing particles. This outgoing state necessarily has $L_z = 0$, implying $S_z = 0$. So the outgoing fermion and anti-fermion have the same helicity, and must arise from different Weyl spinors. The s -wave annihilation matrix element thus violates Standard Model flavor symmetries in the chiral limit, and must be proportional to the Weyl spinor mixing introduced by new physics. As a result, s -wave annihilation is suppressed in scenarios such as MFV, where Weyl spinor mixing vanishes in the chiral limit.

The $L = 1$ initial state, however, can have $S = 1$, $J = 1$; the $J = 1$ fermion/anti-fermion final state can have $S_z = J_z = 1$, implying that the fermion and anti-fermion have opposite helicities and arise from the same Weyl spinor. Thus, the p -wave annihilation matrix element survives in the chiral limit even if there is no Weyl spinor mixing.

However, the s -wave dark matter initial state can annihilate to a fermion/anti-fermion pair if an additional photon is also emitted. In this case, the annihilation matrix element survives in the chiral limit; the $\bar{f}f\gamma$ final state can have $J = 0$ even if f and \bar{f} arise from the same Weyl spinor, due to the angular momentum carried by the photon. Similarly, the s -wave dark matter initial state can annihilate to a $\gamma\gamma$ final state through a one-loop diagram with f and charged mediators running in the loop; this amplitude also survives in the chiral limit (see Figure 2).

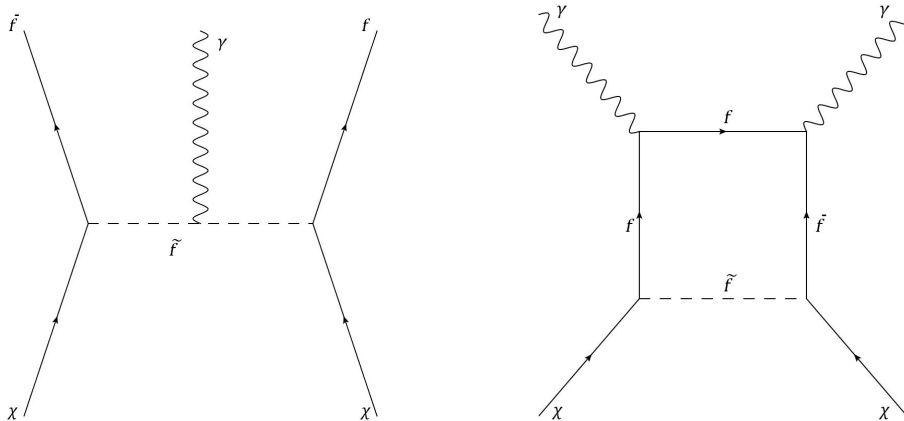


FIG. 2: Representative Feynman diagrams corresponding to the annihilation processes $\chi\chi \rightarrow \bar{f}f\gamma$ (left diagram) and $\chi\chi \rightarrow \gamma\gamma$ (right diagram).

In general, we can express the fermion-photon vertex as

$$\Gamma^\mu(q^2) = \gamma^\mu F_1(q^2) + \frac{i\sigma^{\mu\nu}q_\nu}{2m} F_2(q^2) + \frac{i\sigma^{\mu\nu}\gamma^5 q_\nu}{2m} F_3(q^2) + (\gamma^\mu q^2 - \not{q}q^\mu)\gamma^5 F_A(q^2), \quad (1)$$

where q is the photon momentum and the $F_{1,2,3,A}$ are form factors. The form factors can receive contributions from new physics, including one-loop vertex correction diagrams where χ and the charged mediators run in the loop. One can classify these form factors based on the transformation properties of the various vertex correction terms under C , P , and SM flavor symmetries. In particular, F_2 and F_3 violate SM flavor symmetries by mixing SM Weyl spinors; they must vanish in the chiral limit if there is no Weyl spinor mixing. Both F_1 and F_2 are invariant under C and P separately, while F_3 is CP -odd. F_A is CP -even, but is odd under C and P individually.

We can thus make a general connection between corrections to the various form factors and terms in the $\chi\chi \rightarrow \bar{f}f, \bar{f}f\gamma, \gamma\gamma$ annihilation matrix elements in the chiral limit. The non-relativistic s -wave annihilation matrix element for the process $\chi\chi \rightarrow \bar{f}f$ is necessarily proportional to Weyl spinor mixing, so these terms will be related to corrections to the F_2 and F_3 form factors, and specifically to corrections to the magnetic and electric dipole moments [1]. In particular, the CP -conserving term of the s -wave annihilation matrix element is related to the correction to magnetic dipole moment, while the CP -violating term is related to the electric dipole moment correction. But these terms vanish in the chiral limit if there is no Weyl spinor mixing.

If there is no Weyl spinor mixing, and if C and P are separately conserved, then the only form factor which can receive a correction is F_1 . This correction is then related to the annihilation matrix elements which do not mix SM fermion Weyl spinors, in particular, the p -wave matrix element for the process $\chi\chi \rightarrow \bar{f}f$ and the s -wave matrix elements for the processes $\chi\chi \rightarrow \bar{f}f\gamma, \gamma\gamma$.¹

We can implement the scenario described above with a simplified model, in which χ is a gauge-singlet Majorana fermion which couples to f through the exchange of two scalars, \tilde{f}_L and \tilde{f}_R , via the Lagrangian

$$\mathcal{L} = \lambda\tilde{f}_L(\bar{\chi}P_L f) + \lambda\tilde{f}_R(\bar{\chi}P_R f) + h.c., \quad (2)$$

where λ is a dimensionless coupling constant. We assume that χ and $\tilde{f}_{L,R}$ are odd under a Z_2 symmetry which stabilizes the dark matter. The $\tilde{f}_{L,R}$ have the same quantum numbers as left- and right-handed sfermions, and this simplified model can be used to describe bino-annihilation to $\bar{f}f$ through exchange of sfermions. We further assume that \tilde{f}_L and \tilde{f}_R do not mix and have the same mass ($m_{\tilde{f}} \equiv m_{\tilde{f}_L} = m_{\tilde{f}_R}$). These choices ensure that the annihilation matrix elements respect C and P , and do not mix SM Weyl spinors in the chiral limit.

¹ Note, we do not consider the p -wave matrix elements for the processes $\chi\chi \rightarrow \bar{f}f\gamma, \gamma\gamma$, since they are always suppressed, compared to their s -wave counterparts.

2.1. Annihilation

To lowest order in the relative velocity (v), the annihilation cross section for the process $\chi\chi \rightarrow \bar{f}f$ can be written as (see, for example, [4–6])

$$\langle\sigma_{\bar{f}f}v\rangle = \frac{\lambda^4 N_c r}{12\pi m_{\bar{f}}^2} \frac{1+r^2}{(1+r)^4} \langle v^2 \rangle, \quad (3)$$

where $\langle v^2 \rangle$ is the thermal average of v^2 and $r \equiv m_\chi^2/m_{\bar{f}}^2$ satisfies the constraint $0 < r \leq 1$. Since there is no Weyl spinor mixing, this cross section is necessarily p -wave suppressed. N_c is the number of color states for the fermion f ; $N_c = 1$ if $f = e, \mu, \tau$, while $N_c = 3$ if $f = q$. If the dark matter is a thermal relic, then at the time of freeze-out, one expects $\langle v^2 \rangle \sim 0.1$. But in the current epoch, $\langle v^2 \rangle \sim 10^{-6}$, implying that the $\bar{f}f\gamma$ and $\gamma\gamma$ final states may be important for the purposes of indirect detection.

The differential cross section for the process $\chi\chi \rightarrow \bar{f}f\gamma$ can be written as [7, 8]

$$\begin{aligned} \frac{d\sigma_{\bar{f}f\gamma}}{dx} v = & \frac{\lambda^4 N_c \alpha Q_f^2 r (1-x)}{32\pi^2 m_{\bar{f}}^2} \left[\frac{4x}{(1+r)(1+r-2xr)} - \frac{2x}{(1+r-xr)^2} \right. \\ & \left. + \frac{(1+r)(1+r-2xr)}{r(1+r-xr)^3} \ln \frac{1+r-2xr}{1+r} \right], \end{aligned} \quad (4)$$

where Q_f is the electric charge of f , $x \equiv E_\gamma/m_\chi$, E_γ is the energy of the photon, and $0 \leq x \leq 1$. The total cross section is then given by [4, 8, 9]

$$\begin{aligned} \langle\sigma_{\bar{f}f\gamma}v\rangle = & \frac{\lambda^4 N_c \alpha Q_f^2}{32\pi^2 m_{\bar{f}}^2 r^2} \left[(1+r) \left(\frac{\pi^2}{6} - \ln^2 \frac{1+r}{2} - 2\text{Li}_2 \frac{1+r}{2} \right) \right. \\ & \left. + \frac{3r^2 + 4r}{1+r} + \frac{4 - 3r - r^2}{2} \ln \frac{1-r}{1+r} \right] \end{aligned} \quad (5)$$

We are primarily interested in the limits $r \sim 1$ (when the χ has nearly the same mass as the mediators) and $r \ll 1$ (when the mediators are heavy). We then find

$$\begin{aligned} \langle\sigma_{\bar{f}f\gamma}v\rangle_{r \ll 1} & \sim \frac{\lambda^4 N_c r}{120\pi^2 m_{\bar{f}}^2} (\alpha Q_f^2 r^2), \\ \langle\sigma_{\bar{f}f\gamma}v\rangle_{r \rightarrow 1} & \sim \frac{\lambda^4 N_c}{32\pi^2 m_{\bar{f}}^2} \left[\frac{7}{2} - \frac{\pi^2}{3} \right] \alpha Q_f^2. \end{aligned} \quad (6)$$

The total cross section for the one-loop process $\chi\chi \rightarrow \gamma\gamma$ can be written as [8, 10–12]

$$\langle\sigma_{\gamma\gamma}v\rangle = \frac{\lambda^4 N_c \alpha^2 Q_f^4}{64\pi^3 m_{\bar{f}}^2 r} [\text{Li}_2(r) - \text{Li}_2(-r)]^2, \quad (7)$$

yielding

$$\begin{aligned}\langle\sigma_{\gamma\gamma}v\rangle_{r\ll 1} &\sim \frac{\lambda^4 N_c r}{16\pi^3 m_{\tilde{f}}^2} \alpha^2 Q_f^4, \\ \langle\sigma_{\gamma\gamma}v\rangle_{r\rightarrow 1} &\sim \frac{\lambda^4 N_c \pi}{1024 m_{\tilde{f}}^2} \alpha^2 Q_f^4.\end{aligned}\tag{8}$$

2.2. Correction to the Charge Radius

One can also compute the vertex correction arising from the two diagrams where χ and either \tilde{f}_L or \tilde{f}_R run in the loop. As expected, the only form factor which receives a correction is F_1 . To first order in q^2 , F_1 may be expanded as

$$F_1(q^2) \equiv 1 + \frac{1}{6} q^2 R^2 + \mathcal{O}(q^4),\tag{9}$$

where R is the charge radius (gauge-invariance implies that $F_1(q^2 = 0) = 1$). The vertex correction arising from diagrams with χ and $\tilde{f}_{L,R}$ running in the loop yields a correction to the charge radius given by

$$|\Delta R^2| = \frac{3\lambda^2}{8\pi^2 m_{\tilde{f}}^2} \frac{3r^2 + (1 - 4r) - 2r^2 \ln r}{4(1 - r)^3}.\tag{10}$$

Again, our main interest is in the limits $r \sim 1$ and $r \ll 1$, in which case we find

$$\begin{aligned}|\Delta R^2|_{r\ll 1} &= \frac{3\lambda^2}{32\pi^2 m_{\tilde{f}}^2}, \\ |\Delta R^2|_{r\sim 1} &= \frac{\lambda^2}{16\pi^2 m_{\tilde{f}}^2}.\end{aligned}\tag{11}$$

We thus see that the correction to the charge radius scales as $\Delta R^2 \propto \lambda^2/m_{\tilde{f}}^2$, where the remaining model dependence arises only from rescaling by an $\mathcal{O}(1)$ function of r .

We may then express the relevant annihilation cross sections in terms of ΔR^2 and r as

$$\begin{aligned}\langle\sigma_{\tilde{f}\tilde{f}}v\rangle &= \left[N_c (\Delta R^2)^2 m_{\tilde{f}}^2 r \langle v^2 \rangle \right] \left(\frac{256\pi^3}{27} \left(\frac{(1-r)^3}{3r^2 + (1-4r) - 2r^2 \ln r} \right)^2 \left(\frac{1+r^2}{(1+r)^4} \right) \right), \\ \langle\sigma_{\tilde{f}\tilde{f}\gamma}v\rangle &= \left[N_c (\Delta R^2)^2 m_{\tilde{f}}^2 r^3 \alpha Q_f^2 \right] \left(\frac{32\pi^2}{9} \left(\frac{(1-r)^3}{3r^2 + (1-4r) - 2r^2 \ln r} \right)^2 \left(\frac{1}{r^5} \right) \right) \\ &\quad \times \left[(1+r) \left(\frac{\pi^2}{6} - \ln^2 \frac{1+r}{2} - 2\text{Li}_2 \frac{1+r}{2} \right) + \frac{3r^2 + 4r}{1+r} + \frac{4 - 3r - r^2}{2} \ln \frac{1-r}{1+r} \right], \\ \langle\sigma_{\gamma\gamma}v\rangle &= \left[N_c (\Delta R^2)^2 m_{\tilde{f}}^2 r \alpha^2 Q_f^4 \right] \left(\frac{16\pi}{9} \left(\frac{(1-r)^3}{3r^2 + (1-4r) - 2r^2 \ln r} \right)^2 \right) \left[\frac{\text{Li}_2(r) - \text{Li}_2(-r)}{r} \right]^2\end{aligned}\tag{12}$$

All of these annihilation cross sections scale with the charge radius correction and the mediator mass as $\langle\sigma v\rangle \propto (\Delta R^2)^2 m_{\tilde{f}}^2$; constraints on the annihilation cross section thus become weaker if the mediating particles are heavy. But the cross sections for the processes $\chi\chi \rightarrow \bar{f}f, \bar{f}f\gamma, \gamma\gamma$ scale as r, r^3, r , respectively. These constraints are thus most stringent when the dark matter is much lighter than the mediator, and the mediator is as light as is consistent with experimental constraints.

3. CONSTRAINTS FROM DATA

Searches for sleptons have been performed at LEP [13–16] and the LHC [17, 18], and can be used to place rough lower bounds on $m_{\tilde{f}}$ in the case where $f = e, \mu, \tau$. Consistency with searches at LEP require $m_{\tilde{f}} \gtrsim 100$ GeV, while LHC searches would require $m_{\tilde{f}} \gtrsim 300$ GeV in the $r \rightarrow 0$ limit (these constraints are a little weaker in the $r \rightarrow 1$ limit). In the case where $f = q$, one can estimate lower bounds on $m_{\tilde{f}}$ from LHC squark searches [19]. These bounds would roughly require $m_{\tilde{f}} \gtrsim 500$ GeV in the $r \rightarrow 0$ limit (again, these constraints are somewhat weaker in the $r \rightarrow 1$ limit). As shown in eq. (12), the bound on the annihilation cross section is strongest when $m_{\tilde{f}}$ saturates the lower bound.

The charge radius of SM fermions is constrained at LEP by precise measurements of energy dependence of the $e^+e^- \rightarrow \bar{f}f$ cross section via Drell-Yan production [2]. For this analysis, $f = e, \mu, \tau$, or q , where $q = u, d, s, c, b$ (it is assumed that the charge radius of the quarks is universal). These results are summarized in Table I. Note, in deriving these constraints, it was assumed that the electron and outgoing fermion have the same charge radius; these constraints are thus weakened for $f \neq e$ by a factor $\sqrt{2}$ if the electron is instead taken to be point-like. Comparable constraints on the correction to the quark charge radius have been obtained at HERA [20].

channel	$ \Delta R $
e^+e^-	$< 3.1 \times 10^{-19}\text{m}$
$\mu^+\mu^-$	$< 2.4 \times 10^{-19}\text{m}$
$\tau^+\tau^-$	$< 4.0 \times 10^{-19}\text{m}$
$\bar{q}q$	$< 3.0 \times 10^{-19}\text{m}$

TABLE I: Constraints on the charge radius of Standard Model fermions (e, μ, τ) and quarks (q) obtained from searches at LEP [2].

If $m_{\tilde{f}} \gtrsim 300$ GeV, then a correction to the charge radius which is large enough to be constrained by LEP data would already be close to (if not ruled out by) the perturbativity limit, $\lambda \leq \sqrt{4\pi}$. It is

thus already clear that, given the constraints on charged mediators from the LHC, current charge radius bounds from LEP can only be of limited utility in constraining dark matter annihilation. But future analyses at experiments with higher energy and luminosity could yield much more precise measurements of the charge radius.

For the remainder of this section, we will focus on the case $f = \mu$, $m_{\bar{f}} = 300 \text{ GeV}$ and consider two different scenarios: current muon charge radius bounds from LEP, and the possibility that the bound on the muon charge radius could be improved by a factor of 10 with future experiments. Since the cross section bounds arising from charge radii measurements scale as $\langle \sigma_{\bar{f}f, \bar{f}f\gamma, \gamma\gamma} v \rangle \propto (\Delta R)^4 m_{\bar{f}}^2$, one can easily rescale these bounds for a different choice of $m_{\bar{f}}$, or for future constraints on ΔR . Similarly, the maximum cross section consistent with perturbativity (for any of the channels we have discussed) scales as $\propto m_{\bar{f}}^{-2}$; one can easily rescale the perturbativity limit for a different choice of $m_{\bar{f}}$.

3.1. Thermal Freeze-out

At the time of dark matter thermal freeze-out, one typically expects [21] $\langle v^2 \rangle \sim \mathcal{O}(0.1)$. We can express the $\chi\chi \rightarrow \bar{f}f$ p -wave annihilation cross section as

$$\begin{aligned} \langle \sigma_{\bar{f}f} v \rangle = & (5.5 \times 10^3 \text{ pb}) r N_c \left[\left(\frac{\Delta R^2}{(3 \times 10^{-19} \text{ m})^2} \right)^2 \left(\frac{m_{\bar{f}}}{300 \text{ GeV}} \right)^2 \frac{\langle v^2 \rangle}{0.1} \right] \\ & \times \left(\frac{(1-r)^3}{3r^2 + (1-4r) - 2r^2 \ln r} \right)^2 \left(\frac{(1+r^2)}{(1+r)^4} \right). \end{aligned} \quad (13)$$

In Figure 3, we plot the charge radius constraints on $\langle \sigma_{\bar{f}f} v \rangle$ as a function of r ($m_{\bar{f}} = 300 \text{ GeV}$, $\langle v^2 \rangle = 0.1$). The red long-dashed contour describes the constraints which arise from current bounds on the muon charge radius, while the blue short-dashed contour describes the constraints which would arise if the charge radius were constrained to be 10 times smaller by future data. The regions above the contours are excluded, assuming that there is no other source for corrections to the fermion charge radius. Also plotted is the largest cross section consistent with perturbativity ($\lambda^2 = 4\pi$). We see that, if the precision of fermion charge radius can reach the $\mathcal{O}(10^{-20} \text{ m})$ level for $m_{\bar{f}} \lesssim 3000 \text{ GeV}$, then models in which the dark matter relic density in early Universe is depleted by two-body p -wave annihilation would be correlated with a measurable charge radius correction.

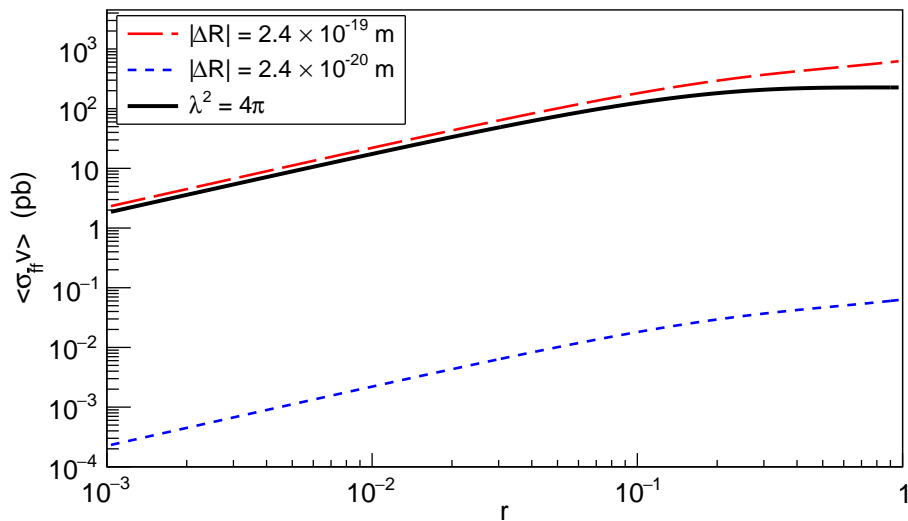


FIG. 3: Bounds on $\langle \sigma_{\bar{f}f} v \rangle$ (in pb) arising from measurements of Standard Model fermion charge radii, where $f = \mu$, $m_{\bar{f}} = 300$ GeV and $\langle v^2 \rangle = 0.1$. The red long-dashed contour corresponds to the case where $\Delta R = 2.4 \times 10^{-19}$ m (the current limit on the muon charge radius correction), and the blue short-dashed contour corresponds to the case where $\Delta R = 2.4 \times 10^{-20}$ m. The region above the curves is excluded, if there are no other corrections to the fermion charge radii. Also shown is the perturbativity limit, $\lambda^2 = 4\pi$ (black solid).

3.2. Indirect Detection in the Current Epoch

In the current epoch, when $\langle v^2 \rangle \sim 10^{-6}$, indirect detection signals arising from the processes $\chi\chi \rightarrow \bar{f}f\gamma$ (internal bremsstrahlung) and $\chi\chi \rightarrow \gamma\gamma$ (via a one-loop diagram) may be competitive with $\chi\chi \rightarrow \bar{f}f$. We may express these cross sections as

$$\begin{aligned}
\langle \sigma_{\bar{f}f\gamma} v \rangle &= (12.8 \text{ pb}) r^3 N_c Q_f^2 \left[\left(\frac{\Delta R^2}{(3 \times 10^{-19} \text{ m})^2} \right)^2 \left(\frac{m_{\bar{f}}}{300 \text{ GeV}} \right)^2 \right] \\
&\quad \times \left(\frac{15}{4} \left(\frac{(1-r)^3}{3r^2 + (1-4r) - 2r^2 \ln r} \right)^2 \left(\frac{1}{r^5} \right) \right) \\
&\quad \times \left[(1+r) \left(\frac{\pi^2}{6} - \ln^2 \frac{1+r}{2} - 2\text{Li}_2 \frac{1+r}{2} \right) + \frac{3r^2 + 4r}{1+r} + \frac{4-3r-r^2}{2} \ln \frac{1-r}{1+r} \right], \\
\langle \sigma_{\bar{\gamma}\gamma} v \rangle &= (0.22 \text{ pb}) r N_c Q_f^4 \left[\left(\frac{\Delta R^2}{(3 \times 10^{-19} \text{ m})^2} \right)^2 \left(\frac{m_{\bar{f}}}{300 \text{ GeV}} \right)^2 \right] \\
&\quad \times \left(\frac{(1-r)^3}{3r^2 + (1-4r) - 2r^2 \ln r} \right)^2 \left(\frac{\text{Li}_2(r) - \text{Li}_2(-r)}{2r} \right)^2. \tag{14}
\end{aligned}$$

Note, we will assume that dark matter couples to only one SM fermion, so there are no interference effects.

In Figures 4 and 5, we plot the charge radius constraints on $\langle\sigma_{\gamma\gamma}v\rangle$ and $\langle\sigma_{\bar{f}f\gamma}v\rangle$, respectively, as functions of r ($m_{\bar{f}} = 300$ GeV). The red long-dashed contour describes the constraints which arise from current bounds on the muon charge radius, while the blue short-dashed contour describes the constraints which would arise if the charge radius were constrained to be 10 times smaller by future data. Again, the regions above the contours are excluded if there are no other sources for corrections to the fermion charge radius, and we also plot the largest cross sections consistent with perturbativity ($\lambda^2 = 4\pi$). In Figure 4, we also plot current observational bounds on $\langle\sigma_{\gamma\gamma}v\rangle$ obtained by Fermi-LAT [23].

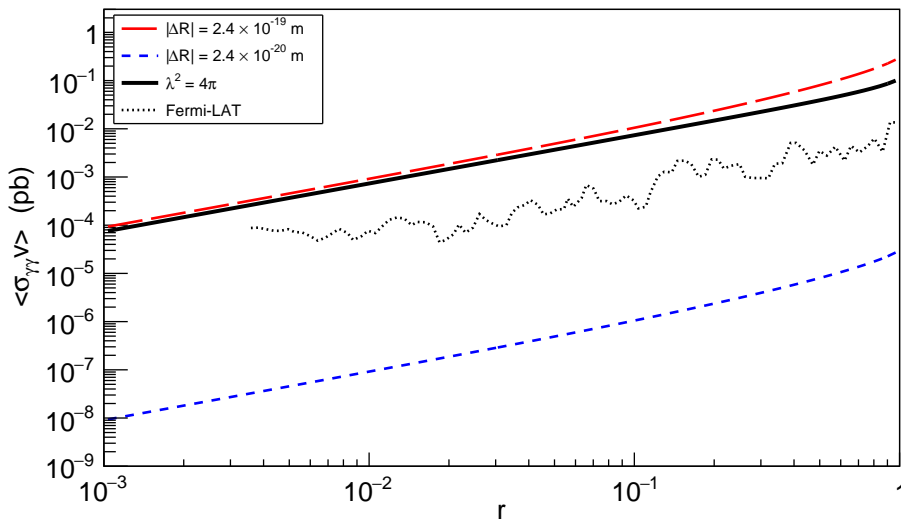


FIG. 4: Bounds on $\langle\sigma_{\gamma\gamma}v\rangle$ (in pb) arising from measurements of Standard Model fermion charge radii, where $f = \mu$ and $m_{\bar{f}} = 300$ GeV. The red long-dashed contour corresponds to the case where $\Delta R = 2.4 \times 10^{-19}$ m (the current limit on the muon charge radius correction), and the blue short-dashed contour corresponds to the case where $\Delta R = 2.4 \times 10^{-20}$ m. The region above the curves is excluded, if there are no other corrections to the fermion charge radii. Also shown is the perturbativity limit (black solid), and observational bounds from Fermi-LAT (black dotted) [23].

The process $\chi\chi \rightarrow \gamma\gamma$ can proceed from an s -wave initial state, but $\langle\sigma_{\gamma\gamma}v\rangle$ is suppressed by a factor $\alpha^2 \sim \mathcal{O}(10^{-4})$. This cross section will be somewhat larger than $\langle\sigma_{\bar{f}f\gamma}v\rangle$ in the current epoch. Moreover, because this annihilation process produces monoenergetic photons, the signal is much more easily detected above background. As a result, this process will be much more important than $\chi\chi \rightarrow \bar{f}f$ for indirect detection in the current epoch. For $m_{\bar{f}} \sim 300$ GeV, we find that constraints on the $\chi\chi \rightarrow \gamma\gamma$ annihilation process arising from fermion charge radii measurements could exceed current constraints from Fermi-LAT by more than three orders of magnitude (absent fine-tuning),

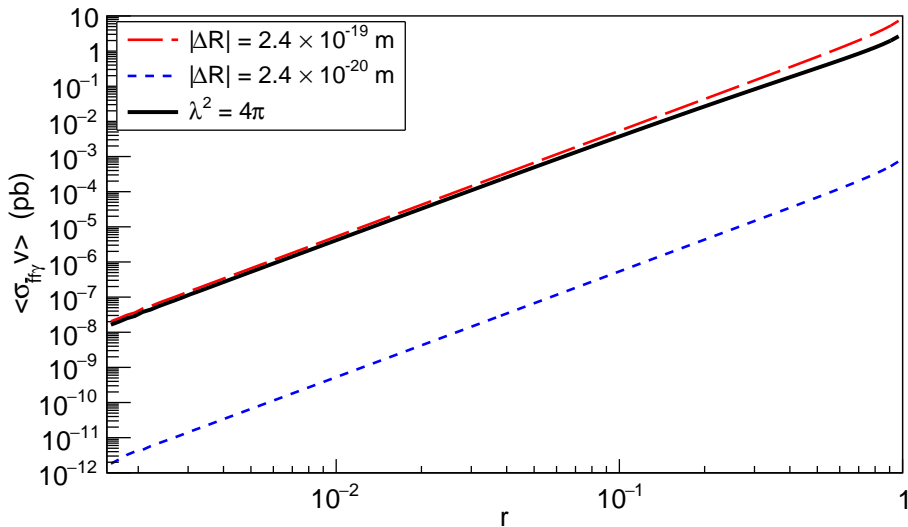


FIG. 5: Bounds on $\langle \sigma_{\bar{f}f\gamma} v \rangle$ (in pb) arising from measurements of Standard Model fermion charge radii, where $f = \mu$ and $m_{\bar{f}} = 300 \text{ GeV}$. The red long-dashed contour corresponds to the case where $\Delta R = 2.4 \times 10^{-19} \text{ m}$ (the current limit on the muon charge radius correction), and the blue short-dashed contour corresponds to the case where $\Delta R = 2.4 \times 10^{-20} \text{ m}$. The region above the curves is excluded, if there are no other corrections to the fermion charge radii. Also shown is the perturbativity limit (black solid).

if the charge radii corrections could be measured at the $\mathcal{O}(10^{-20} \text{ m})$ level.

Dark matter annihilation via internal bremsstrahlung is an s -wave process, but instead receives a factor αr^2 suppression. For $r \sim 1$, however, the photon spectrum arising from internal bremsstrahlung is very hard; the photon spectrum is similar in shape to a line signal, implying that the IB cross section can also be constrained by line signal searches using Fermi-LAT [23]. For $m_{\bar{f}} \sim 300 \text{ GeV}$, fermion charge radii constraints on $\langle \sigma_{\bar{f}f\gamma} v \rangle$ could surpass Fermi-LAT constraints on IB in the nearly-degenerate limit by up to two orders of magnitude, if the charge radii can be measured at the $\mathcal{O}(10^{-20} \text{ m})$ level.

For $r < 1$, however, the photon spectrum will be smooth, and the sensitivity of Fermi-LAT and other indirect detection experiments will be significantly weaker. Measurements of the fermion charge radii at the $\mathcal{O}(10^{-20} \text{ m})$ level would thus provide an even more dramatic improvement over current indirect detection results. But for $r \lesssim \mathcal{O}(0.1)$, however, we see that indirect detection prospects will in any case tend to be dominated by the process $\chi\chi \rightarrow \gamma\gamma$.

4. CONCLUSIONS

We have seen that measurements of Standard Model fermion charge radii can be used to constrain cross sections for dark matter annihilation in scenarios where dark matter couples to SM fermions through a charged mediator, and where helicity mixing is suppressed. In particular, the p -wave cross section for the process $\chi\chi \rightarrow \bar{f}f$, and s -wave cross sections for the internal bremsstrahlung process $\chi\chi \rightarrow \bar{f}f\gamma$ and the one-loop process $\chi\chi \rightarrow \gamma\gamma$, can be constrained by measurements of fermion charge radii. However, it is always possible for other new physics, unrelated to dark matter, to produce canceling corrections to the charge radius, allowing a large annihilation cross section to be consistent with experimental data. As such, the bounds we have found do not correspond to a rigorous limit, but rather demarcate the rough point at which fine-tuning would be needed in order to retain consistency with the data.

It is worth noting that the annihilation processes $\chi\chi \rightarrow \bar{f}f\gamma, \gamma\gamma$ can only proceed if dark matter couples to SM fermions through an interaction mediated by a charged particle. There will thus always be a correction to the fermion-photon vertex arising from a one-loop diagram where dark matter and the charged mediators run in the loop. Thus, the correlation between the fermion charge radius correction and the $\chi\chi \rightarrow \bar{f}f\gamma, \gamma\gamma$ annihilation cross sections is robust.

Unfortunately, current measurements of the fermion charge radii from LEP are not precise enough to yield useful constraints on dark matter annihilation. But future experiments such as VHEeP [24] and ILC could provide much tighter constraints on the SM fermion charge radii. As the annihilation cross sections scale as $(\Delta R)^4$, even a modest improvement in charge radii constraints would correspond to a dramatic improvement in constraints on the dark matter annihilation cross section. For example, a high-luminosity run at VHEeP could yield an improvement in charge radii measurements of an order of magnitude [24], resulting in an improvement in bounds on dark matter annihilation of $\mathcal{O}(10^{-4})$. Such a dramatic improvement would result in constraints which essentially exceed all current observational bounds for all of the channels which we have considered over the entire range of r at $m_{\bar{f}} \sim 300$ GeV. High-luminosity e^+e^- colliders would be ideally suited for this type of study [25].

5. ACKNOWLEDGEMENT

We are grateful to Tom Browder, Bhaskar Dutta, Danny Marfatia and Sven Vahsen for useful discussions. JK is supported in part by NSF CAREER grant PHY-1250573.

-
- [1] K. Fukushima and J. Kumar, Phys. Rev. D **88**, no. 5, 056017 (2013) doi:10.1103/PhysRevD.88.056017 [arXiv:1307.7120].
 - [2] M. Acciarri *et al.* [L3 Collaboration], Phys. Lett. B **489**, 81 (2000) doi:10.1016/S0370-2693(00)00887-X [hep-ex/0005028].
 - [3] J. Kumar and D. Marfatia, Phys. Rev. D **88**, no. 1, 014035 (2013) doi:10.1103/PhysRevD.88.014035 [arXiv:1305.1611 [hep-ph]].
 - [4] N. F. Bell, J. B. Dent, A. J. Galea, T. D. Jacques, L. M. Krauss and T. J. Weiler, Phys. Lett. B **706**, 6 (2011) doi:10.1016/j.physletb.2011.10.057 [arXiv:1104.3823 [hep-ph]].
 - [5] A. Pierce, N. R. Shah and K. Freese, arXiv:1309.7351 [hep-ph].
 - [6] K. Fukushima, C. Kelso, J. Kumar, P. Sandick and T. Yamamoto, Phys. Rev. D **90**, no. 9, 095007 (2014) doi:10.1103/PhysRevD.90.095007 [arXiv:1406.4903 [hep-ph]].
 - [7] T. Bringmann, L. Bergstrom and J. Edsjo, JHEP **0801**, 049 (2008) doi:10.1088/1126-6708/2008/01/049 [arXiv:0710.3169 [hep-ph]].
 - [8] J. Kumar, P. Sandick, F. Teng and T. Yamamoto, Phys. Rev. D **94**, no. 1, 015022 (2016) doi:10.1103/PhysRevD.94.015022 [arXiv:1605.03224 [hep-ph]].
 - [9] K. Fukushima, Y. Gao, J. Kumar and D. Marfatia, Phys. Rev. D **86**, 076014 (2012) doi:10.1103/PhysRevD.86.076014 [arXiv:1208.1010 [hep-ph]].
 - [10] L. Bergstrom and P. Ullio, Nucl. Phys. B **504**, 27 (1997) doi:10.1016/S0550-3213(97)00530-0 [hep-ph/9706232].
 - [11] Z. Bern, P. Gondolo and M. Perelstein, Phys. Lett. B **411**, 86 (1997) doi:10.1016/S0370-2693(97)00990-8 [hep-ph/9706538].
 - [12] P. Ullio and L. Bergstrom, Phys. Rev. D **57**, 1962 (1998) doi:10.1103/PhysRevD.57.1962 [hep-ph/9707333].
 - [13] A. Heister *et al.* [ALEPH Collaboration], Phys. Lett. B **544**, 73 (2002) doi:10.1016/S0370-2693(02)02471-1 [hep-ex/0207056].
 - [14] P. Achard *et al.* [L3 Collaboration], Phys. Lett. B **580**, 37 (2004) doi:10.1016/j.physletb.2003.10.010 [hep-ex/0310007].
 - [15] J. Abdallah *et al.* [DELPHI Collaboration], Eur. Phys. J. C **31**, 421 (2003) doi:10.1140/epjc/s2003-01355-5 [hep-ex/0311019].
 - [16] G. Abbiendi *et al.* [OPAL Collaboration], Eur. Phys. J. C **32**, 453 (2004) doi:10.1140/epjc/s2003-01466-

- y [hep-ex/0309014].
- [17] G. Aad *et al.* [ATLAS Collaboration], JHEP **1405**, 071 (2014) doi:10.1007/JHEP05(2014)071 [arXiv:1403.5294 [hep-ex]].
 - [18] V. Khachatryan *et al.* [CMS Collaboration], Eur. Phys. J. C **74**, no. 9, 3036 (2014) doi:10.1140/epjc/s10052-014-3036-7 [arXiv:1405.7570 [hep-ex]].
 - [19] G. Aad *et al.* [ATLAS Collaboration], JHEP **1409**, 176 (2014) doi:10.1007/JHEP09(2014)176 [arXiv:1405.7875 [hep-ex]].
 - [20] H. Abramowicz *et al.* [ZEUS Collaboration], Phys. Lett. B **757**, 468 (2016) doi:10.1016/j.physletb.2016.04.007 [arXiv:1604.01280 [hep-ex]].
 - [21] Ya. B. Zeldovich, Adv. Astron. Astrophys. **3**, 241 (1965); H.Y. Chiu, Phys. Rev. Lett. **17**, 712 (1966); G. Steigman, Ann. Rev. Nucl. Part. Sci. **29**, 313 (1979); R.J. Scherrer and M.S. Turner, Phys. Rev. D **33**, 1585 (1986).
 - [22] C. Kelso, J. Kumar, P. Sandick and P. Stengel, Phys. Rev. D **91**, 055028 (2015) doi:10.1103/PhysRevD.91.055028 [arXiv:1411.2634 [hep-ph]].
 - [23] M. Ackermann *et al.* [Fermi-LAT Collaboration], Phys. Rev. D **91**, no. 12, 122002 (2015) doi:10.1103/PhysRevD.91.122002 [arXiv:1506.00013 [astro-ph.HE]].
 - [24] A. Caldwell and M. Wing, Eur. Phys. J. C **76**, no. 8, 463 (2016) doi:10.1140/epjc/s10052-016-4316-1 [arXiv:1606.00783 [hep-ex]].
 - [25] J. A. Aguilar-Saavedra *et al.* [ECFA/DESY LC Physics Working Group Collaboration], hep-ph/0106315.